ResearchGate

See discussions, stats, and author profiles for this publication at: https://www.researchgate.net/publication/230923982

Comparison of Empirical Models for Polar and Equatorial Coronal Holes

Article *in* The Astrophysical Journal · December 2008

DOI: 10.1086/319166

CITATIONS
22

READS
48

5 authors, including:

A. V. Panasyuk
Harvard-Smithsonian Center for Astrophysics
76 PUBLICATIONS **2,007** CITATIONS
SEE PROFILE

Marco Romoli
University of Florence
214 PUBLICATIONS **2,902** CITATIONS
SEE PROFILE

Some of the authors of this publication are also working on these related projects:

ESA-NASA Solar Orbiter Mission - Metis Coronagraph View project

ADAHELI+ View project

All content following this page was uploaded by Marco Romoli on 21 April 2015.

The user has requested enhancement of the downloaded file.

THE ASTROPHYSICAL JOURNAL, 549:L257–L260, 2001 March 10
© 2001. The American Astronomical Society. All rights reserved. Printed in U.S.A.

COMPARISON OF EMPIRICAL MODELS FOR POLAR AND EQUATORIAL CORONAL HOLES

M. P. MIRALLES,[1] S. R. CRANMER,[1] A. V. PANASYUK[1] M. ROMOLI,[2] AND J. L. KOHL[1]

Received 2000 October 23; accepted 2001 January 23; published 2001 March 6

ABSTRACT

We present a self-consistent empirical model for several plasma parameters of a large equatorial coronal hole observed on 1999 November 12 near solar maximum. The model was derived from observations with the Ultraviolet Coronagraph Spectrometer on the *Solar and Heliospheric Observatory*. In this Letter, we compare the observations of O VI λλ1032, 1037 emission lines with previous observations of a polar coronal hole observed near solar minimum. At the time of the 1999 observations, there was no evidence of large polar coronal holes. The resulting empirical model for the equatorial coronal hole describes the outflow velocities and most probable speeds for O^{5+}, and we compared the derived ion properties with the empirical model for a solar minimum polar coronal hole. The comparison of the empirical models shows that the 1999 equatorial hole has lower O^{5+} outflow speeds and perpendicular temperatures than its polar counterpart from 1996 to 1997 at heights between 2 and 3 $R_\odot$. However, in situ asymptotic speeds of the wind streams coming from the 1996–1997 polar hole and from the 1999 equatorial hole are only ~15% different. Thus, the bulk of the solar wind acceleration must occur above 3 $R_\odot$ for the equatorial coronal hole. The equatorial hole also has a higher density than the polar hole at similar heights. It is not yet known whether the higher densities are responsible for the seeming inhibition of the fast ion outflow speeds and extremely large perpendicular temperatures that occur in polar coronal holes at solar minimum. We discuss the constraints and implications on various theoretical models of coronal heating and acceleration.

Subject headings: line: profiles — solar wind — Sun: corona — Sun: UV radiation — techniques: spectroscopic

1. INTRODUCTION

Coronal holes are known sources of the fast solar wind (Krieger, Timothy, & Roelof 1973). At solar minimum, coronal holes that form over the north and south heliographic poles are relatively stable structures observed to exist for several years. During active phases of the solar cycle, the large polar holes disappear and smaller, more short-lived holes form at various latitudes. An extensive empirical model for a polar coronal hole (at solar minimum) was presented by Kohl et al. (1998) and Cranmer et al. (1999). In this Letter, we present an empirical model of a large equatorial hole present during the rising phase of solar cycle 23, when the Sun was approaching the maximum of solar activity. The equatorial coronal hole was correlated with high-speed wind streams with velocities ~600–700 km s^{-1}, as measured by the *Advanced Composition Explorer* (*ACE*) spacecraft when the hole was oriented in its direction. The ultraviolet emission line observations were conducted during 1999 November 11–14 using the Ultraviolet Coronagraph Spectrometer (UVCS) aboard the *Solar and Heliospheric Observatory* (*SOHO*). The UVCS instrument is described by Kohl et al. (1995). At the time of the observations, there was no evidence of either north or south polar coronal holes in the National Solar Observatory (NSO)/Kitt Peak He I λ10830 disk images. The main body of the equatorial hole was a diagonal structure of ~30° in longitude and ~20° in latitude. Solar differential rotation did not seem to affect strongly the overall diagonal shape of the equatorial hole, indicating near-rigid rotation of the corona over several months.

This Letter provides spectroscopic diagnostics of O^{5+} velocity distributions and outflow velocities derived from measurements of intensities and line widths for O VI λλ1032, 1037 as a function of height and latitude in an equatorial coronal hole. The resulting empirical model for the plasma properties of the equatorial hole is then compared with the empirical model for a polar coronal hole observed near solar minimum.

In the remainder of this Letter, we outline the UVCS observations that are incorporated into the empirical model (§ 2), construct a detailed picture of the dynamics of coronal O^{5+} ions (§ 3), and discuss the implications of the empirical data and the comparison of theoretical models of polar and equatorial coronal holes (§ 4).

2. UVCS OBSERVATIONS OF THE EQUATORIAL CORONAL HOLE

The large equatorial coronal hole that we studied persisted over more than six solar rotations, from 1999 October to 2000 March. It could be seen clearly both on the solar disk (when aligned with the Earth) and in the extended corona (when in the plane of the sky) over this time period. Figure 1*a* shows a representative image of the corona when the hole was on the west equatorial limb at the time of our observations.

The UVCS instrument on *SOHO* was used to measure intensities and line profiles for the O VI λλ1032, 1037 doublet. UVCS observations were made for approximately 24 hr each day during the period 1999 November 11–14. Five projected heliocentric heights were observed once each day: 1.6, 1.8, 2.1, 2.6, and 3.1 $R_\odot$. The average integration times were 3600, 5400, 12,600, 18,000, and 43,200 s, respectively. The nominal slit position angles were 261° (at 1.6 $R_\odot$) and 265° (at 3.1 $R_\odot$) measured counterclockwise from the north heliographic pole. The instrument configuration for the observations included an entrance slit of 75 μm for the O VI channel, a spatial binning of 3 pixels (21″), a spectral binning of 2 pixels (0.185 Å), and an instantaneous field of view of 40′ × 21″. The procedure for correcting the UVCS observations for instrumental effects is described in more detail by Kohl et al. (1997, 1999) and A. V. Panasyuk et al. (2001, in preparation). We used the UVCS Data Analysis Software (DAS) in combination with the line profile fitting codes developed by A. V. Panasyuk et al. (2001,

[1] Harvard-Smithsonian Center for Astrophysics, 60 Garden Street, MS 50, Cambridge, MA 02138; mmiralles@cfa.harvard.edu.
[2] Universitá di Firenze, Dipartimento di Astronomia e Scienza dello Spazio, Largo Enrico Fermi 5, Firenze 50125, Italy.

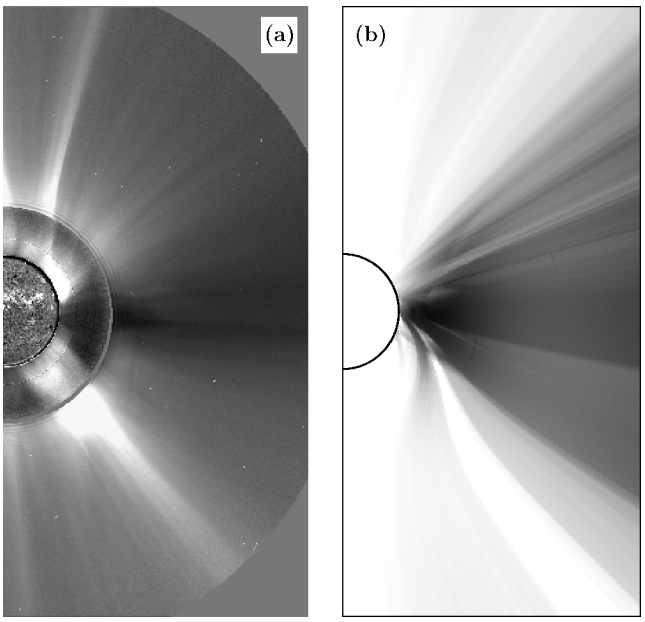

FIG. 1.—(*a*) White-light *pB* composite image of the corona observed on 1999 November 12 between 17:00 and 22:00 UT. The solar corona images were taken with (*middle image*) the ground-based Mauna Loa Solar Observatory/HAO Mark IV and (*outermost image*) the LASCO C2/*SOHO* coronagraphs. The Hα image of the solar disk was taken with (*innermost image*) the ground-based BBSO telescopes. (*b*) Synthesized image of the white-light *pB* in the empirical model. The large equatorial coronal hole (dark region in the image) is visible above the west limb.

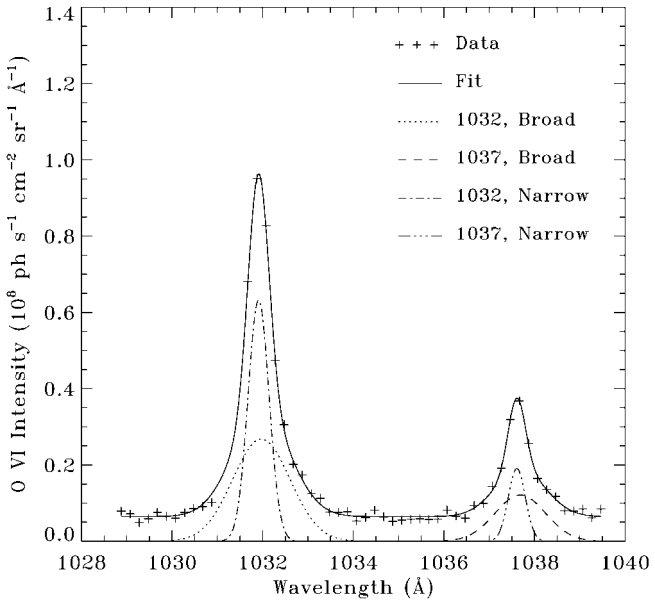

FIG. 2.—UVCS/*SOHO* 1999 November 12 observations of O VI λ1032 and λ1037 profiles for the equatorial coronal hole above the west limb at 21:00 UT, at a heliocentric distance of 2.58 $R_\odot$. Curve fits for two Gaussians plus a constant background are shown for each of the two lines. The data points are shown by crosses, and the fitted profile by a solid line. The best-fit $V_{1/e}$ for the broad coronal profiles are 254 (1032 Å; *dotted line*) and 222 km s^{-1} (1037 Å; *dashed line*) and for the narrow coronal profiles are 80 (1032 Å; *dot-dashed line*) and 59 km s^{-1} (1037 Å; *dash–triple-dotted line*).

in preparation) for flat-field and background correction, wavelength and intensity calibration, and removal of image distortion and stray light (Gardner et al. 1996; Kohl et al. 1997). We measured the total intensities and 1/*e* widths of the O VI emission lines by fitting multiple Gaussian functions to the observed profiles with an algorithm that minimizes the reduced χ^2. The uncertainties in the O VI λλ1032, 1037 line intensities are due to photon counting statistics, background subtraction, and radiometric calibration (estimated to be $\pm$12%–15% at 1 σ) (Gardner et al. 1996).

Figure 2 shows an example of an observed profile at 2.58 $R_\odot$ at the center of the equatorial coronal hole, averaged over an 8′ spatial bin, on 1999 November 12. The integration time was 4.3 hr. Curve fits for two Gaussians plus a constant background are shown for each of the two lines. All parameters of the Gaussian fit were kept free except for the wavelength separation between the line centers of the 1032 Å line. This separation was fixed to be the same as the relative line-center difference between the 1037 Å Gaussians because of the presence of a detector wire on a small region of the short-wavelength side of the 1032 Å line (which adversely affected the data in that region). The profile shows broad wings. We can distinguish two components in the profile: a broad coronal profile corresponding to the equatorial hole and a narrow coronal profile corresponding to the foreground and background streamers. This identification is justified by looking at the line profiles along the slit. The profiles show only the narrow component when looking outside the equatorial hole where only the streamer contribution exists. However, toward the part of the slit that is looking directly into the hole, the profile also shows the broad component. The broad component is identified with the equatorial hole. We see these wings only when looking at the hole and when the hole is in the plane of the sky. The narrow and broad components do not have the same line centers, which can be attributed to different bulk Doppler shifts of the volumes responsible for the two components.

Figure 3 shows the comparison of the polar and equatorial coronal holes' total line-integrated intensities for O VI λ1032 and O VI λ1037, and the O VI intensity ratio (1032 Å intensity divided by 1037 Å intensity). Below 2 $R_\odot$, the O VI intensities are similar for both holes. Above 2 $R_\odot$, however, the equatorial hole intensities are a factor of 3 brighter and the O VI intensity ratios are 1.5 times higher. Because the 1999 equatorial hole subtends a smaller portion of the line of sight than the 1996–1997 polar hole and is still brighter, the local *emissivities* in the equatorial hole must be larger than those of the polar hole by significantly more than the factor of 3 difference in the intensities.

3. IONIZED OXYGEN EMPIRICAL MODELS

We construct an *empirical model* of the equatorial coronal hole in order to determine its plasma parameters (temperatures, velocities, densities). This model is a three-dimensional description of the plasma parameters that reproduces the observed data when input into a radiative transfer line synthesis code. It is important to emphasize that the empirical models described here do not specify the processes that maintain the coronal plasma in its assumed steady state. Thus, there is no explicit mention of coronal heating and acceleration mechanisms, waves and turbulent motions, and magnetic field structure, within the models themselves. The iterated quantities in the models depend on only observations and well-established theory, such as the radiative transfer inherent in the line formation process. A similar empirical model for a polar coronal hole (at solar minimum) was presented by Kohl et al. (1998) and Cranmer et al. (1999).

Because the equatorial coronal hole did not subtend the entire

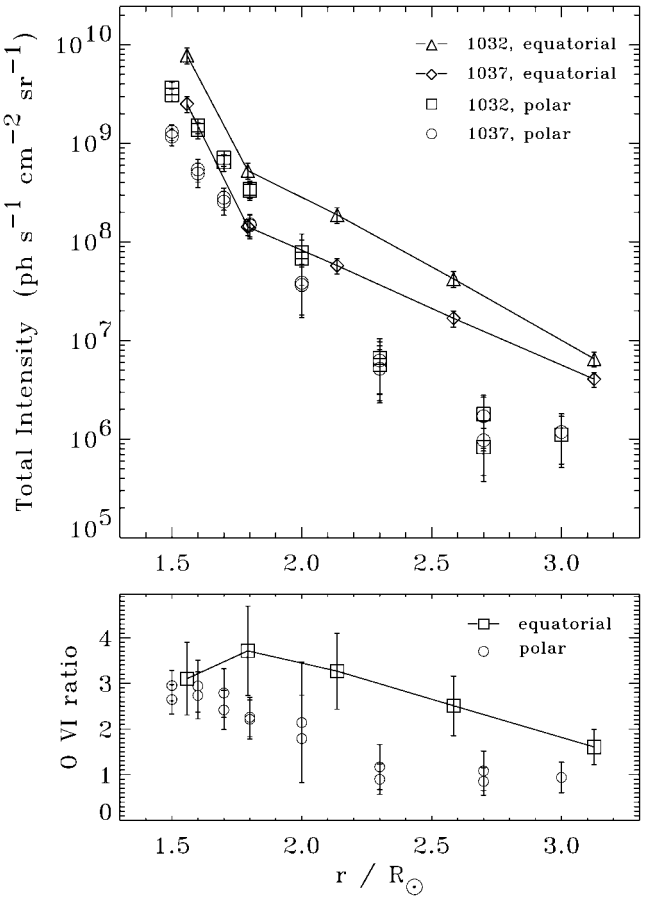

FIG. 3.—Comparison of (*top*) the polar and equatorial coronal holes' O VI total line-integrated intensities and (*bottom*) ratios between O VI λ1032 and λ1037 line intensity. O VI λ1032 intensities for polar (*squares*) and equatorial (*triangles, solid line*) holes and O VI λ1037 intensities for polar (*circles*) and equatorial (*diamonds, solid line*) holes are shown. O VI λ1032 and λ1037 line intensity ratio for polar (*circles*) and equatorial (*squares*) holes are also shown.

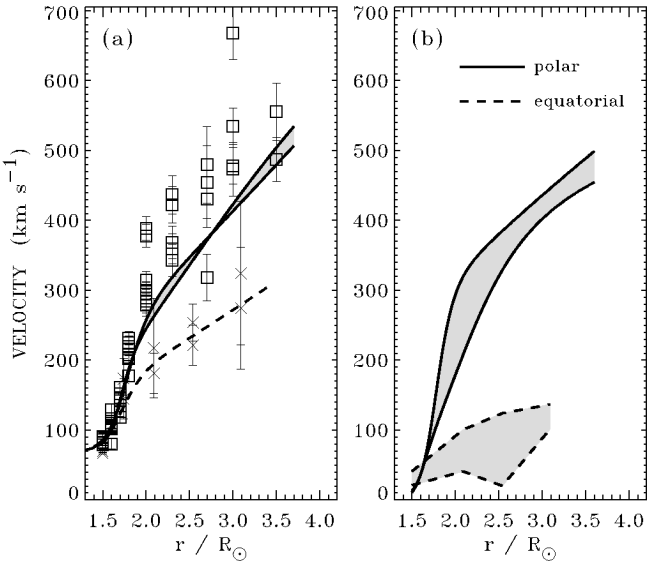

FIG. 4.—(*a*) O VI λλ1032, 1037 radial dependence of $V_{1/e}$ line width velocity in polar (*squares*) and equatorial (*crosses*) coronal holes. Also plotted are the modeled perpendicular most probable speeds. (*b*) Empirical O^{5+} outflow velocities for the polar (*solid lines*) and equatorial (*dashed lines*) holes, derived from O VI intensities and widths.

line of sight of the UVCS observations, the empirical model had to account for the properties of the foreground and background plasma as well. The first step in the modeling process was thus to define the exact volumes of the coronal hole and the surrounding regions. The coronal hole "footprint" on the solar surface was defined using the NSO/Kitt Peak tracings of He I λ10830 emission (e.g., Dunn & Smartt 1991). The holes were assumed to expand outward superradially, using the empirical function of Kopp & Holzer (1976), with $f_{\max} = 6$. The boundaries of the hole were defined with respect to five radial axes placed in central regions of the hole footprints on the surface, and the overall shape of the coronal hole volume was found to be insensitive to the locations and number of these axes. The radial dependence of the electron density n_e, both inside the coronal hole volume and in the surrounding regions, was constrained using several days of UVCS White-Light Channel measurements of the Thomson-scattered polarization brightness (*pB*). As the coronal hole rotated in and out of the plane of the sky, the relative decrease and increase in *pB* allowed the densities in the two regions to be determined. Figure 1*b* shows a reconstruction of the *pB* using the best-fit model parameters for the geometry and density.

The properties of the O^{5+} ions were constrained by modeling the line widths and intensity ratios of the O VI lines observed by UVCS. The broad and narrow Gaussian components of the lines were found to probe reliably the coronal hole and surrounding regions, respectively. As has been found for other coronal structures with nearly radial magnetic fields, the line widths are most sensitive to the perpendicular most probable speed $w_\perp$ of the velocity distribution and the O VI λ1032/λ1027 intensity ratios are most sensitive to the outflow speed u. We assumed lower and upper limits for two other parameters that affect the spectral line synthesis only weakly: (1) the parallel most probable speed $w_\parallel$ in the coronal hole, which was varied between a lower limit of thermal equilibrium with the electron temperature [$w_\parallel = (2kT_e/m_{\rm ion})^{1/2}$] and an upper limit of an isotropic distribution ($w_\parallel = w_\perp$), and (2) the outflow speed in the surrounding regions u_s, which was varied between zero (assuming a closed-loop streamer) and the modeled value of u in the hole. The models were also found to be insensitive to the absolute value of n_e, and varying this quantity by a factor of 3 did not significantly alter the results. There were thus a total of eight models constructed by independently varying $w_\parallel$, u_s, and n_e between lower and upper limits, and the variations in the resulting values of $w_\perp$ and u for the coronal hole represent liberal uncertainties in the modeling process.

4. DISCUSSION AND CONCLUSIONS

Outflow speeds u and perpendicular most probable speeds $w_\perp$ have been derived for the 1999 November equatorial coronal hole. Figure 4*a* plots both $w_\perp$ and the 1/*e* half-widths of the O VI line profiles ($V_{1/e}$) that most strongly constrained the determination of $w_\perp$. The data and empirical models for polar coronal holes in 1996–1997 are also shown. Figure 4*b* shows the empirical O^{5+} outflow speeds for both types of holes, with the gray regions denoting the modeling uncertainties discussed above. Note that when u exceeds 200–300 km s^{-1} the line widths are significantly broadened by outflow components along the line of sight, thus making $V_{1/e} > w_\perp$. This complication does not seem to arise for the equatorial coronal holes, which have O^{5+} outflow speeds about 3–4 times lower than those of the 1996–1997 polar holes. The present result is consistent with

Buchlin & Hassler (2000), who observed blueshifts at the base of this equatorial hole that suggest the wind emanating from this region is about 3 times slower than in their previous polar coronal hole observations (Hassler et al. 1999).

In situ measurements of the wind speed, of about 700–800 km s^{-1}, associated with polar coronal holes were obtained near solar minimum by the *Ulysses* spacecraft (Goldstein et al. 1996). In the case of the 1999 November equatorial coronal hole, the speeds of the associated solar wind streams observed by the *ACE* spacecraft were about 600–700 km s^{-1}. These high-speed streams encountered *ACE* on 1999 November 6–11 and exhibited significant decreases in both the O^{7+}/O^{6+} ionization fraction and the Mg/O abundance ratio. Such properties have been shown to correlate well with streams originating in coronal holes (Zurbuchen et al. 1999). The specific correlation between the equatorial coronal hole observed in 1999 November and the *ACE* high-speed stream was confirmed by T. Zurbuchen (2000, private communication). The *ACE* wind speeds are similar to the ones reported by Nolte et al. (1976) in equatorial holes of comparable size. However, these wind speeds are larger than the ones reported for low-latitude holes of smaller size, between 300 and 600 km s^{-1}, near solar minimum (Neugebauer et al. 1998).

From the coronal observations made by UVCS, we found that the 1999 equatorial coronal hole has 3–4 times lower O^{5+} outflow speeds than its polar counterpart from 1996–1997 at heights between 2 and 3 $R_\odot$. However, the in situ measurements discussed above show that the asymptotic speeds of the wind streams coming from the 1996–1997 polar hole and from the 1999 equatorial hole are similar (only a ~15% difference). Thus, the bulk of the solar wind acceleration must occur above 3 $R_\odot$ for the equatorial coronal hole.[3]

The 1999 equatorial coronal hole has properties that seem to bridge the gap between polar coronal holes and streamers. The derived values of $w_\perp$ and u in the equatorial hole are smaller than those in a polar coronal hole by about a factor of 2–4 above 2 $R_\odot$. The equatorial hole $w_\perp$ speeds are about 2 times larger than those in a solar minimum equatorial streamer above 2 $R_\odot$, but the outflow speeds u are of the same order as those derived in streamers (Strachan et al. 2000). Ongoing analysis of UVCS white-light *pB* measurements also seems to indicate that the electron density in the equatorial hole is several times larger than that in a polar hole but still smaller than that in a streamer (see, e.g., Romoli et al. 1993, 1997; M. Romoli et al. 2001, in preparation). Coulomb collisions are thus more efficient in the equatorial hole (compared with the polar hole) at equilibrating temperatures and outflow speeds of different particle species. Above about 2.5 $R_\odot$, both the polar and equatorial holes are practically collisionless (i.e., the mean collision times are longer than the wind expansion times), but the *absolute* collision rates are significantly faster in the equatorial hole. Studies of proton isotropization in the collisionless solar wind at 1 AU (Griffel & Davis 1969; Livi & Marsch 1987) have shown that relatively small numbers of collisions are necessary to affect the properties of ion velocity distributions. Thus, collisions could be responsible for the lower values of $w_\perp$ and u in the equatorial hole, but it also seems likely that different types of coronal holes have intrinsically different heating and acceleration rates as well. Hollweg (1999) suggested that open-field regions with larger areas on the solar surface should be heated more strongly because of a larger available ion cyclotron wave flux. Observations of coronal holes of different sizes, geometries, and densities may thus be key to understanding how the various types of solar wind plasma are heated and accelerated.

[3] This direct comparison of outflow speeds does not involve assumptions about solar wind acceleration mechanisms or magnetic field divergence. It is probable that both polar and equatorial coronal holes exhibit comparable superradial divergence.

This work is supported by NASA under grant NAG5-7822 to the Smithsonian Astrophysical Observatory, by the Italian Space Agency, and by PRODEX (Swiss contribution). The ground-based polarization brightness image used here was produced by the Mauna Loa Solar Observatory operated by the High Altitude Observatory (HAO). HAO is a division of the National Center for Atmospheric Research, which is sponsored by the National Science Foundation. The space-based polarization brightness image used here is courtesy of the LASCO/*SOHO* consortium. *SOHO* is a project of international cooperation between ESA and NASA. The NSO/Kitt Peak data used here are produced cooperatively by NSF/NOAO, NASA/GSFC, and NOAA/SEL. The Big Bear Solar Observatory (BBSO) is operated by NJIT.

REFERENCES

Buchlin, E., & Hassler, D. M. 2000, BAAS, 32, 810
Cranmer, S. R., et al. 1999, ApJ, 511, 481
Dunn, R. B., & Smartt, R. N. 1991, Adv. Space Res., 11(5), 139
Gardner, L. D., et al. 1996, Proc. SPIE, 2831, 2
Goldstein, B. E., et al. 1996, A&A, 316, 296
Griffel, D. H., & Davis, L. 1969, Planet. Space Sci., 17, 1009
Hassler, D. M., Dammasch, I. E., Lemaire, P., Brekke, P., Curdt, W., Mason, H. E., Vial, J.-C., & Wilhelm, K. 1999, Science, 283, 810
Hollweg, J. V. 1999, J. Geophys. Res., 104, 24781
Kohl, J. L., et al. 1995, Sol. Phys., 162, 313
———. 1997, Sol. Phys., 175, 613
———. 1998, ApJ, 501, L127
———. 1999, ApJ, 510, L59
Kopp, R. A., & Holzer, T. E. 1976, Sol. Phys., 49, 43
Krieger, A. S., Timothy, A. F., & Roelof, E. C. 1973, Sol. Phys., 29, 505
Livi, S., & Marsch, E. 1987, J. Geophys. Res., 92, 7255
Neugebauer, M., et al. 1998, J. Geophys. Res., 103, 14587
Nolte, J. T., et al. 1976, Sol. Phys., 46, 303
Romoli, M., et al. 1993, Appl. Opt., 32, 3559
———. 1997, in The Corona and Solar Wind near Minimum Activity, Fifth *SOHO* Workshop, ed. A. Wilson (ESA SP-404; Noordwijk: ESA), 633
Strachan, L., Panasyuk, A. V., Dobrzycka, D., Kohl, J. L., Noci, G., Gibson, S. E., & Biesecker, D. A. 2000, J. Geophys. Res., 105, 2345
Zurbuchen, T., Hefti, S., Fisk, L. A., Gloeckler, G., & von Steiger, R. 1999, Space Sci. Rev., 87, 353

View publication stats